Electronic Supplementary Material (ESI) for Nanoscale.

High resolution imaging of 3D stray-field components with a scanning Fe_3O_4-nanoparticle sensor

Yan Qi[1], Yihong Kan[1], Zhenghua Li[1*]

[1]Key Laboratory of New Energy and Rare Earth Resource Utilization of State Ethnic Affairs Commission, School of Physics and Materials Engineering, Dalian Minzu University, Dalian, 116600, China

[*]**Corresponding authors**: lizhenghua@dlnu.edu.cn

Section 1. The description of 3D stray-field components

Due to the discontinuous distribution of magnetization (or accumulation of magnetic charges) in samples, the magnetic stray-field will emanate from the magnetic domains or domain walls (Appl. Phys. Lett. 76, 3094–3096). The stray-field vectors ($\vec{H}_d$) above the sample surface can be decomposed into three orthogonal components of $\vec{H}_{dx}$, $\vec{H}_{dy}$, and $\vec{H}_{dz}$, which points along the three orthogonal directions of x, y, and z axis, respectively. Therefore, the "stray-field components" indicate the three orthogonal components of $\vec{H}_{dx}$, $\vec{H}_{dy}$, and $\vec{H}_{dz}$.

Section 2. The description of the micro-coils

In the Fe_3O_4-nanoparticle based MFM system, both micro-coils have been driven by the AC voltage and used for reversing the magnetization of MFM tip. As depicted in Figure 1, when using the micro-coil at the top side, the magnetic moments of the Fe_3O_4-nanoparticle tip will rotate periodically along the film normal direction (out-of-plane), therefore, the Fe_3O_4-nanoparticle can be capable of detecting the out-of-plane component of the stray fields; Similarly, by using the micro-coil at the left side of the probe, the magnetization of the tip will reverse periodically along the x axis (in-film-plane), accordingly, the MFM tip should be sensitive to the in-plane component of the stray fields.

Section 3. The frequency modulation (FM) of the cantilever resonance

In this work, we develop a Fe_3O_4-nanoparticle based sensor technique to locally observe the magnetic fine structures. This technique uses the frequency modulation (FM) of the cantilever resonance. An alternating field (driving frequency of ω_m)

from a micro-coil periodically rotates the magnetic moment of a Fe_3O_4 tip, causing an alternating force between the MFM tip and sample. The alternating force can periodically modulate the effective spring constant of the cantilever, the motion equation of the MFM tip can be given by

$$m\frac{d^2z(t)}{dt^2} + m\gamma\frac{dz(t)}{dt} + (k_0 + \Delta k)z(t) = F_0\cos(\omega_0 t) \qquad \text{(S1)}$$

where z , m , γ and k_0 are the displacement, effective mass , damping factor , and intrinsic spring constant of the MFM tip, respectively. Here, Δk represents the periodic change in the effective spring constant due to AC magnetic force (modulation frequency ω_m), and $F_0\cos(\omega_0 t)$ denotes the oscillating force driven by a piezoelectric element (driven frequency ω_0 equals the resonant frequency of an MFM cantilever). When a MFM tip behaves as a dipole type tip, Δk was given by

$$\begin{aligned}\Delta k &= \frac{\partial F_z}{\partial z} \approx M_z^{ac}\frac{\partial^2 H_z}{\partial z^2}\cos(\omega_m t) + M_x^{ac}\frac{\partial^2 H_x}{\partial z^2}\sin(\omega_m t) \\ &= \Delta k_1\cos(\omega_m t) + \Delta k_2\sin(\omega_m t)\end{aligned} \qquad \text{(S2)}$$

where M_z^{ac} , M_x^{ac} are the amplitudes of the tip magnetization in orthogonal directions, H_z and H_x are the magnetic fields perpendicular and parallel to film plane.

When $\Delta k << k_0$, the narrow-band FM of the cantilever displacement occurs in the following expression:

$$z(t) = \frac{F_0}{m\gamma\omega_0}\sin\left[\omega_0 t + \frac{\Delta k_1}{m\gamma\omega_0}\cos(\omega_m t) + \frac{\Delta k_2}{m\gamma\omega_0}\sin(\omega_m t)\right]$$
$$\approx \frac{F_0}{m\gamma\omega_0}\left(\begin{array}{l}\sin(\omega_0 t) + \frac{\Delta k_1}{2m\gamma\omega_0}\{\cos[(\omega_0+\omega_m)t] + \cos[(\omega_0-\omega_m)t]\} \\ + \frac{\Delta k_2}{2m\gamma\omega_0}\{\sin[(\omega_0+\omega_m)t] - \sin[(\omega_0-\omega_m)t]\}\end{array}\right) \quad \text{(S3)}$$

Figure S1 shows a FM phenomenon in the tip oscillation by applying a modulation frequency of ω_m. From the spectra of the tip oscillation, we can clearly observe two spectra peaks with a frequency of $\omega_0 \pm \omega_m$ near the base-band spectrum (ω_0) of the cantilever oscillation, indicating that the off-resonant AC magnetic force can periodically modulate the effective spring constant of the cantilever. Based on the FM technique, the modulated MFM signal (ω_0 - ω_m) gradually decays with the increase of the modulation frequency f_m ($\omega_m = 2\pi f_m$), when f_m reaches 1 kHz, the MFM signal is too weak to be detected, therefore, the maximum measured frequency is limited to 1 kHz.

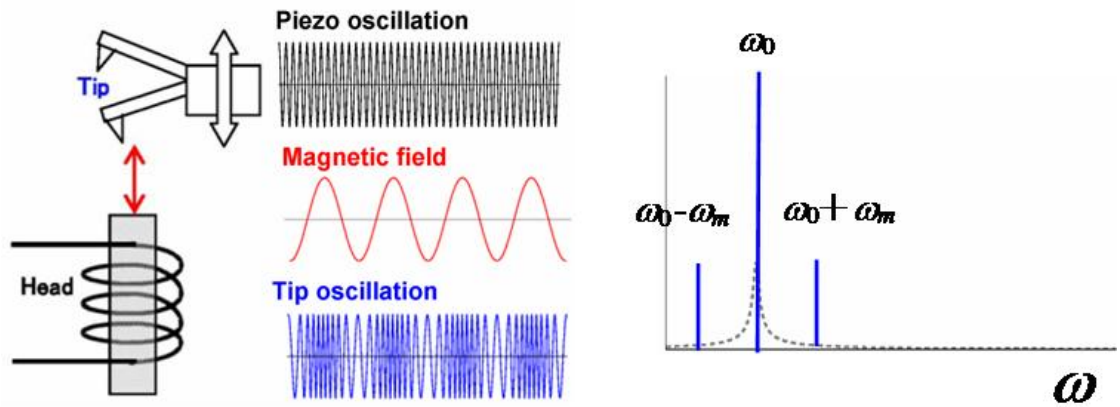

Figure S1. The principle of frequency modulation (FM).

Section 4. The Fe_3O_4-nanoparticle based MFM image vs. modulation frequency

The Fe_3O_4-nanoparticle based MFM uses the frequency modulation (FM) of the cantilever resonance (Nanoscale 2014, 6 (19), 11163), the maximum detectable frequency of the Fe_3O_4-nanoparticle based MFM is 1 kHz. The present MFM technique relies on the mixing of two frequencies, one is the modulation frequency f_m, and other one is the resonant frequency f_0 of the tip cantilever. The measured MFM signal depends on the difference between two frequencies ($|f_0 - f_m|$, see Supporting Materials, Section 3). With the increase of modulation frequency f_m, the measured MFM signal gradually decays obeying the law of frequency modulation. Figure S2 depicts the MFM image of FePt perpendicular magnetic recording medium vs. modulation frequency f_m. As seen in Figure S2, with the increase of f_m from 125 Hz to 1 kHz, the MFM signal gradually decays, and nearly disappears at the f_m of 1 kHz. Therefore, the maximum detectable frequency of this MFM technique can be extended to 1 kHz.

Figure S2. The Fe_3O_4-nanoparticle based MFM image of FePt perpendicular magnetic recording medium. The black bars represent 100 nm.

Section 5. The magnetic imaging theories of Fe_3O_4-nanoparticle based MFM

In the Fe_3O_4-nanoparticle based MFM, the MFM tip oscillations can be described as

$$m\frac{d^2z(t)}{dt^2} + m\gamma\frac{dz(t)}{dt} + (k_0 + \Delta k)z(t) = F_0\cos(\omega_0 t) \qquad \text{(S4)}$$

here z , γ , m and k_0 are the displacement, damping constant, effective mass and intrinsic stiffness of the oscillated MFM tip. Δk is the periodic change in the effective spring constant of the MFM tip, and $F_0 \cos(\omega_0 t)$ is an alternating force from piezo-electric elements.

An AC voltage V(ω_m) is applied to a micro-coil to produce a modulated H-field, which can periodically transform the magnetization directions of Fe_3O_4-nanoparticle, the magnetization $\vec{M}_{\text{tip}}^{ac}(t)$ of tip rotates periodically,

$$\vec{M}_{\text{tip}}^{ac}(t) = \vec{M}_z(t) + \vec{M}_x(t) = M_z^{ac}\cos(\omega_m t)\vec{\text{j}} + M_x^{ac}\sin(\omega_m t)\vec{\text{i}} \qquad \text{(S5)}$$

here M_z^{ac} , M_x^{ac} are the amplitudes of tip magnetization perpendicular and parallel to sample surface, respectively.

The MFM tip behaves as magnetic dipole-type tip, the magnetic force between ($\vec{\text{F}}_z$) tip and sample is defined as:

$$\vec{\text{F}}_z = -\frac{\partial}{\partial \text{z}}(\vec{\text{M}}_{\text{tip}}^{\text{ac}} \cdot \vec{\text{H}})\,\vec{\text{j}} = -[M_z^{ac}\frac{\partial H_z}{\partial z}\cos(\omega_m t) + M_x^{ac}\frac{\partial H_x}{\partial z}\sin(\omega_m t)]\vec{\text{j}} \qquad \text{(S6)}$$

here H_z and H_x are the perpendicular and in-plane components of magnetic fields from sample surface, respectively.

The measured MFM signals are proportional to the first derivative of the magnetic force （$\frac{\partial F_z}{\partial \text{z}}$）, thus, the periodic change in the effective spring constant of the Fe_3O_4-tip can be described as

$$\begin{aligned}\Delta k = \frac{\partial F_z}{\partial z} &\propto M_z^{ac}\frac{\partial^2 H_z}{\partial z^2}\cos(\omega_m t) + M_x^{ac}\frac{\partial^2 H_x}{\partial z^2}\sin(\omega_m t) \\ &= \Delta k_1 \cos(\omega_m t) + \Delta k_2 \sin(\omega_m t)\end{aligned} \qquad \text{(S7)}$$

Base on lock-in technique, the in-phase (X) and out-of-phase (Y) signals, corresponding to the sine and cosine parts in equation (S7), can be extracted as

$$X + iY \propto \Delta k_1 \cos(\omega_m t) + i\Delta k_2 \sin(\omega_m t) \quad \text{(S8)}$$

Meanwhile, the amplitude (A) and phase (P) signals can also be extracted by lock-in technique:

$$A = [\Delta k_1^2 + \Delta k_2^2]^{1/2} \quad \text{(S9)}$$

$$P = \arctan[\Delta k_2 / \Delta k_1] \quad \text{(S10)}$$

Section 6. The description of the micromagnetic model

In the micromagnetic simulation, standard parameters of FeCo materials are selected: saturation magnetization of 1.4 MA/m, crystalline anisotropy constant of 4×10^2 J/m^3, exchange stiffness of 18 pJ/m, and damping coefficient of 0.5. The energy terms include Zeeman, crystalline anisotropies, shape anisotropies, magnetic exchanges, and magnetostatic energies:

$$E^i{}_{total} = E^i{}_{Zee} + E^i{}_{ck} + + E^i{}_{sk} + E^i{}_{ex} + E^i{}_m \quad \text{(S11)}$$

The effective field $\vec{H}^i_{eff}$ is defined as :

$$\vec{H}^i_{eff} = -\frac{1}{\mu_0}\frac{\partial E^i}{\partial \vec{M}^i} \quad \text{(S12)}$$

Where $\vec{M}^i$ is the magnetization in *i*th grid.

The reversals of magnetic moments obey the law of Landau–Lifshitz–Gilbert (LLG) equations:

$$\frac{d\vec{M}^i}{dt} = -\gamma\vec{M}^i \times \vec{H}^i{}_{eff} - \frac{\alpha}{M_s}\vec{M}^i \times (\vec{M}^i \times \vec{H}^i{}_{eff}) \quad \text{(S13)}$$

where *Ms* , γ and α present the saturation magnetization, gyromagnetic coefficient, and damping constant, respectively.

Section 7. The magnetic imaging of domain walls inside the vortices

The vortex structure with a polarized core at center lead to a spatially distributed MFM contrast, due to the formation of magnetic domain walls inside a vortex structure. This statement can be evidenced by the MFM images of vortices formed in FeCo disk, square pad and triangle dot, as seen in Figure S3. For magnetic vortices with in-plane oriented spins, the MFM only senses magnetic field that originated from the domain walls rather than the domain themselves. In the case of FeCo circular disk, no domain wall exists inside the circular-shaped vortex, and the MFM result only presents the polarity of one vortex core. However, in the case of square or triangle shape, domain walls form inside vortex due to the breaking of circular symmetry and generating of demagnetization field from square or triangle corners, therefore, the MFM results present the distribution of magnetic field originated from domain walls. The chirality of vortex can be identified by the direction of magnetic dipoles, as marked by arrows (from dark to bright) in Figure S3.

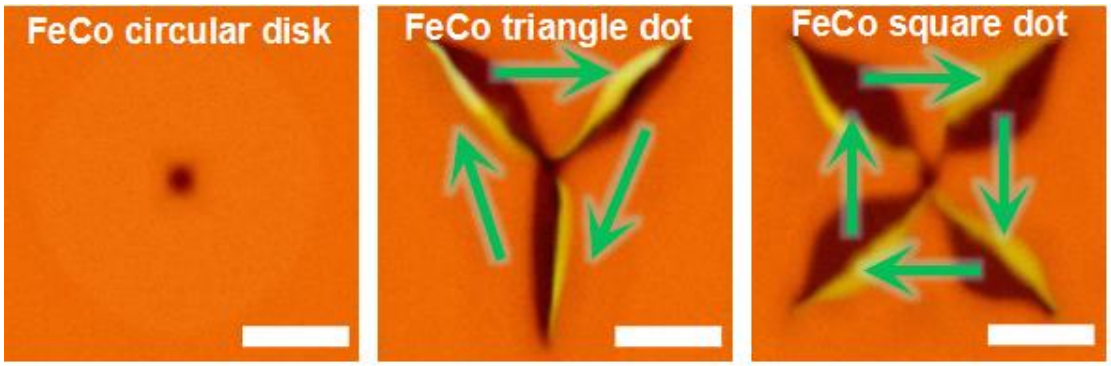

Figure S3**.** MFM images of FeCo disk, square pad and triangle dot. The while colour bars represent 100 nm.

Section 8. The analysis of the spatial resolution

we have performed the Fourier-based analysis to prove the resolution of 5 nm. The spatial resolution can be determined by a Fourier-based analysis of the MFM signals (J. Appl. Phys. 83, 5609-5620). Figure S4 depicts the response of the MFM signal (along the horizontal centerline of Figure 3(k)) from a magnetic vortex as a function of spatial frequency (k_x). In the Fourier spectrum of Figure S4, the MFM resolution can be evaluated by the maximum detectable frequency (k_c), where the intensity of MFM signal spectrum reduces to the white background level (thermodynamic noise of cantilever) (J. Appl. Phys. 83, 5609-5620; IEEE Trans. Magn. 40, 2194-2196; IEEE Trans. Magn. 39, 3447-3449). As seen in Figure S4, the critical frequency $k_c \approx 100$ （1/μm）, the resolution can be estimated as half of the critical wavelength $\lambda_c = \frac{1}{2k_c} \approx 5.0$ nm.

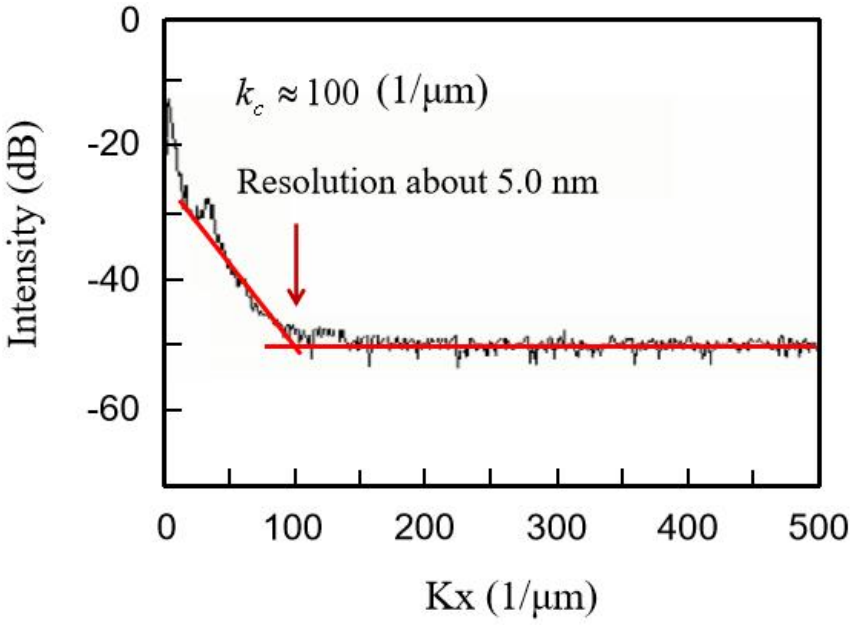

Figure S4. Fourier spectrum of the MFM signal

The factors of determining the spatial resolution: the performance of MFM tip (nanosized tip apex, optimized magnetic coating, etc), the tip-to-sample distance, the

signal-to-noise ratio, and the extreme measuring conditions (ultra-low temperature and ultra-high vacuum). In order to improve the spatial resolution, we use a small Fe_3O_4 nanoparticle tip (about 10 nm) , reduce the tip-sample distance, separate the magnetic and atomic phases (Supporting Materials, Section 9), and enhance the signal to noise ratio by a lock-in technique. For further enhancing the resolution, we should further optimize the performance of MFM tip (reduce the tip apex of less than 5 nm, optimize the magnetic coating, design the geometrical shape etc), precise control the tip-to-sample distance near surface, gradually improve the measuring conditions (ultra-low temperature and ultra-high vacuum), to break through the spatial resolution on the order of atomic scales.

Section 9. Separation of the magnetic and atomic phases

Figure S5 depicts the Fe_3O_4-nanoparticle based MFM image and the relating conventional MFM image for a FePt perpendicular magnetic recording medium. As shown in Figure S5, we can get high quantity MFM images with small tip-sample distance (very near surface). However, at the same experimental conditions, conventional phase-detection MFM did not produce a clear image, because the magnetic force is weaker than the short-range atomic forces arising from the surface. Therefore，the Fe_3O_4-nanoparticle based MFM can separate the magnetic and atomic phases and obtain high spatial resolution.

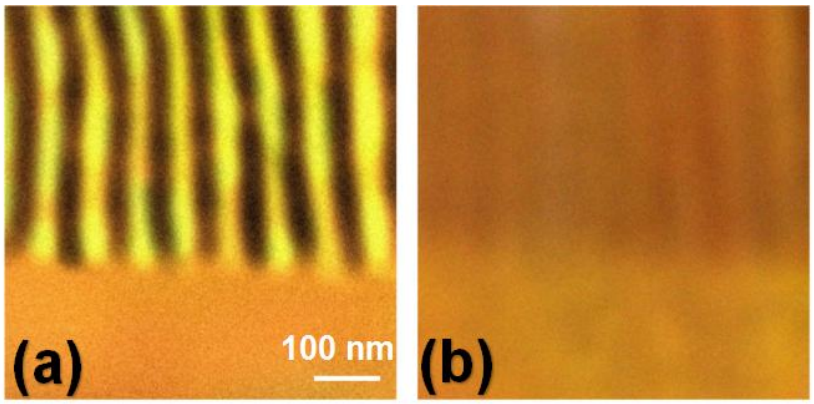

Figure S5. (a) Fe_3O_4-nanoparticle based MFM image, (b) conventional MFM for a FePt perpendicular magnetic recording medium.